Soft Matter

The effects of protein charge patterning on complex coacervation

Journal:	*Soft Matter*
Manuscript ID	SM-ART-04-2021-000543.R1
Article Type:	Paper
Date Submitted by the Author:	08-Jun-2021
Complete List of Authors:	Zervoudis, Nicholas; Columbia University, Chemical Engineering Obermeyer, Allie; Columbia University, Chemical Engineering

The effects of protein charge patterning on complex coacervation

*Nicholas A. Zervoudis, Allie C. Obermeyer**

Department of Chemical Engineering, Columbia University, New York, NY 10027

Abstract

The complex coacervation of proteins with other macromolecules has applications in protein encapsulation and delivery and for determining the function of cellular coacervates. Theoretical or empirical predictions for protein coacervates would enable the design of these coacervates with tunable and predictable structure-function relationships; unfortunately, no such theories exist. To help establish predictive models, the impact of protein-specific parameters on complex coacervation were probed in this study. The complex coacervation of sequence-specific, polypeptide-tagged, GFP variants and a strong synthetic polyelectrolyte was used to evaluate the effects of protein charge patterning on phase behavior. Phase portraits for the protein coacervates demonstrated that charge patterning dictates the protein's binodal phase boundary. Protein concentrations over 100 mg mL^{-1} were achieved in the coacervate phase, with concentrations dependent on the tag polypeptide sequence covalently attached to the globular protein domain. In addition to shifting the binodal phase boundary, polypeptide charge patterning provided entropic advantages over isotropically patterned proteins. Together, these results show that modest changes of only a few amino acids in the tag polypeptide sequence alter the coacervation thermodynamics and can be used to tune the phase behavior of polypeptides or proteins of interest.

Introduction.

Membraneless compartments in eukaryotic cells, such as the nucleolus, Cajal bodies, and stress granules, have been observed for centuries.[1–4] However, in the last decade, understanding of the underlying molecular interactions that govern the formation and behavior of these phase separated microcompartments has dramatically improved.[2,5–8] It has been speculated that many membraneless organelles comprised of proteins and nucleic acids phase separate into two coexisting immiscible phases via complex coacervation, a liquid-liquid phase separation phenomenon driven by electrostatic interactions between oppositely-charged polyelectrolytes.[9–17] These dense liquid compartments are dynamic, retain material exchange with their environment, and exhibit selectivity in the macromolecules that they encapsulate.[18–20] Biologically, the phase transitions of proteins (and other biopolymers) are essential for intracellular organization, and have demonstrated functions such as regulating RNA and protein homeostasis, responding to heat shock, and enhancing cellular signaling processes.[21–24] In addition to the role in normal cell physiology, biomolecular condensates are implicated in disease progression, such as the formation of protein aggregates observed in neurodegenerative diseases.[24–28]

Phase transitions of macromolecules are also ubiquitous in nonliving systems. Particularly, in polymer sciences, understanding and controlling phase transitions has enabled considerable progress in membrane technologies, porous glasses, composites, and thermo-electrics.[29–33] As the fundamental understanding of the phase behavior of synthetic polymers has progressed, efforts have turned to sequence-defined biopolymers such as proteins.[34–36] Similarly to synthetic macromolecules, understanding the phase behavior of proteins has potential to enable applications in the biotechnology domain, namely in protein isolation and protein delivery systems.[20,37–39] Complex coacervates can encapsulate high concentrations of

protein[37] (~ 200 mg mL^{-1}) with increased stability to organic solvents,[40] proteases,[41] ionic strength,[41,42] and time.[43] In addition to protein stabilization, complex coacervates have also been shown to increase the activity of encapsulated enzymes.[42,44] Developing the proper design rules to tune protein complex coacervation would enable novel opportunities in biomedicine and biocatalysis, while also potentially providing molecular-level insights into the relationship between protein sequence and membraneless organelle formation.

A predictive framework for the associative phase separation of globular protein biopolymers would enable the rational design of this behavior. For example, existing theories for simple coacervation of synthetic polymers or intrinsically disordered proteins (IDPs), such as elastin-like polypeptides (ELPs), have facilitated the rational design and tunable control of the phase behavior of these macromolecules.[17,45–51] In polymer physics, describing course-grained effective interactions with a χ parameter is often a sufficient descriptor of the structure-function relationship of a polymer in a particular solvent.[46,47,52] Similarly, design rules have been established for ELPs that have enabled a structure-function relationship between canonical biopolymer sequences and their respective lower critical solution temperatures (LCST).[48,49] Unfortunately, analogous structure-function relationships for globular protein phase separation via complex coacervation remain unresolved. Complex coacervation of linear polyelectrolytes has been accurately and theoretically described using adaptations of the Voorn-Overbeek liquid lattice model of polymer solutions.[16,17,53–55] This original model developed a quantitative theoretical treatment for the entropy of mixing and electrostatic attraction by combining the Debye-Huckel equations for electrical interactions and the Flory-Huggins equations for entropy.[15–17] Adaptations by de Pablo,[55,56] Ganesan,[57,58] Wang,[59–61] Olvera de la Cruz[62,63], and Sing[53,64] have accounted for polymer chain connectivity, excluded

volume interactions, and charge fluctuations to develop a comprehensive and quantitative description of the phase behavior of simple, flexible polyelectrolytes and colloids. As described by Sing et. al., non-mean field theoretical adaptations are necessary to resolve the small and complex molecular-length scale correlations that are critical for describing coacervate equilibrium dynamics in flexible, charged polymers.[53,64] However, globular proteins represent a more complicated subset of polyelectrolytes due to their ampholytic nature and relatively fixed secondary structure. In order to develop robust theoretical predictions, additional experimental data relating protein-specific properties, such as charge patterning and conformational heterogeneity, to phase behavior are needed. Various macromolecular properties modulate a protein's ability to form favorable interactions and ultimately phase separate.[65] While weaker, non-electrostatic interactions such π-π stacking, cation-π, and hydrophobic interactions are often essential to intracellular phase separation, manipulating the charge and charge patchiness of a protein via protein engineering or chemical modifications is a simple and effective strategy that can be used to promote coacervation.[65–68] Additionally, several studies have shown that proteins with intrinsically disordered regions (IDRs) are more likely to phase separate.[27,69,70] IDRs or IDPs are composed of polypeptide segments lacking the ability to cooperatively fold and form a stable tertiary structure.[71] These proteins and protein regions are often characterized by a high proportion of polar or charged amino acids and have been shown to drive phase separation of membraneless organelles.[12,71–73] Critically, it has been observed that the sequence of intrinsically disordered or synthetic polypeptides impacts the phase behavior.[12,51,71–74] Recent work from Perry and Sing has demonstrated the sequence-dependent complex coacervation of linear polypeptides, where the repeat length, or blockiness, of charged and neutral amino acids governed the thermodynamic driving force for

phase separation.[73–76] Here, a similar strategy was employed for globular proteins with polypeptide tags consisting of charged and neutral residues. Charge patterning was achieved through the use of short polypeptide tag sequences that were expected to complement with the larger globular domain to demonstrate the interplay and relative importance of the two domains. The polypeptide tag charge blockiness was varied in an attempt to tune the binodal phase boundary of GFP variants and a strong polyelectrolyte as a function of salt concentration (Figure 1A).

With these considerations, a library of protein mutants was created to determine the effects of protein charge density and charge patterning on complex coacervation (Figure 1B). This was done by genetically fusing charged tags onto the C-terminus of superfolder GFP (sfGFP). The tag polypeptide sequences consisted of ionizable aspartate (D) and glutamate (E) and neutral glycine (G) and serine (S) residues. The polypeptides charge density, patterning, and lengths were varied in order to assess the effect of charge patchiness on complex coacervation when coupled with an inherently patchy globular protein domain. The tags exist as a source of structural disorder that was expected to promote phase separation as previously demonstrated with other IDRs. To narrow the large parameter space, the complex coacervation of these sfGFP variants was investigated with a single strong synthetic polyelectrolyte (quaternized poly(4-vinyl *N*-methyl pyridinium iodide). The balance between the globular protein (sfGFP) and ionic polypeptide tags with varying sequence enables evaluation of the relative importance of phase separation design criteria such as electrostatic interactions, entropy gains from the release of condensed counterions, and conformational heterogeneity. Here, we demonstrate that both charge and charge patterning dictate the protein's binodal phase boundary as a function of salt (NaCl) concentration. Additionally, protein concentrations

over 100 mg mL^{-1} were achieved in the dense coacervate phase. This high protein concentration was maintained at elevated ionic strengths in a sequence-dependent manner, with blockier sequences promoting higher protein concentrations in the coacervate phase. Differences in the thermodynamics of complex coacervation were also investigated by isothermal titration calorimetry (ITC) and revealed that coacervation was driven by sequence specific entropic gains as has been seen in polypeptide-based complex coacervates.

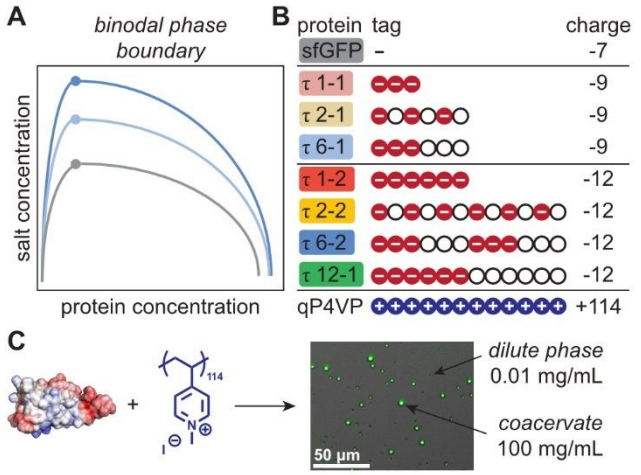

Figure 1. (A) Qualitative illustration of a typical phase portrait for complex coacervate forming (bio)macro-molecules. (B) Schematic of the sequence defined polypeptide materials used in this study. (C) Representative example of the complex coacervation of an anionic GFP variant (τ 6-2) with qP4VP. Fluorescence microscopy image of the condensed phase with no added salt and protein concentration in the coacervate and dilute phases at low salt conditions.

Results.

A library consisting of sfGFP and 7 polypeptide tagged variants were designed and biosynthesized to analyze the effects of polypeptide charge patterning on the complex coacervation of globular proteins. The polypeptide tags were designed to have a net charge of -3 or -6 and were fused to the C-terminus of sfGFP. The net charge for each variant was calculated using the isolated amino acid side chain pK_a for Asp, Arg, Glu, and Lys. The naming convention was defined according to the polypeptide sequence periodicity, τ, and numbers *x*-*y*,

where *x* corresponds to the periodicity, and *y* corresponds to the number of repeat units. Ultimately, this resulted in eight protein variants with three possible theoretical net charges at pH 7.4: -7 (▲ sfGFP), -9 (■ τ 1-2, τ 2-1, τ 6-1), and -12 (● τ 1-2, τ 2-2, τ 6-2, τ 12-1). Additionally, an isotropically charged variant, GFP(-12), was used as a control for protein net charge in the binodal composition assays and thermodynamic analysis.

GFP variants were expressed in *E. coli* and purified via Ni-NTA affinity chromatography. Purified samples were characterized via MALDI-TOF and gel electrophoresis (Figure S1 and S2). While the central goal of appending polypeptide tags onto the globular protein domain was to tune the protein's phase behavior, for this approach to be practical, it was essential that the charged tags did not affect protein biosynthesis. Cell growth kinetics and protein expression for each mutant were quantified by monitoring optical density at 600 nm (OD_{600}) and total cell fluorescence, respectively (Figure S3 and S4). Cell growth and protein expression were not affected by the addition of charged polypeptide tags on the C-terminus of sfGFP, indicating that this method of protein supercharging does not impose additional stress on the cell or affect protein yields.

Preliminary phase separation assays were performed to determine the relative mixing ratios of protein and quaternized poly(4-vinyl *N*-methyl pyridinium iodide) (qP4VP) that maximize phase separation and incorporation of GFP in the coacervate phase. The results of these preliminary coacervation assays are summarized in Table S1. The turbidity at 600 nm was used as a marker for phase separation of each mutant when mixed with the strong polycation qP4VP. All of the GFP mutants phase separated at low ionic strength with a maximum turbidity of approximately 90%. Turbidity values were plotted as a function of negative charge fraction (Figure S5A). For simple polyelectrolyte systems, the expected

maximum in turbidity would occur at a charge fraction of 0.5.[77–79] For this protein-polyelectrolyte system, turbidity maximums were observed at f^- ~ 0.2, indicating that an excess of polymer is required relative to the theoretically optimal charge neutral mixing ratios. This shift is thought to be specific to protein systems as ionizable amino acids may undergo induced charging in the presence of cationic polymer.[67,80,81] While turbidity was used as a marker of phase separation, optical microscopy was used to distinguish the morphological nature of the resulting phases; the phase separated protein and polymer mixtures formed dense, liquid-like coacervate phases (Figure S6iv). At the negative charge fraction corresponding to maximum turbidity, all of the tagged GFP variants were efficiently incorporated in the coacervate phase at conditions of low ionic strength (Figure S5B). In other words, charge distribution had minimal impact on the phase separation at low ionic strength.

Ionic strength is an important factor governing complex coacervation.[15,82,83] To evaluate the salt dependence of coacervation for each mutant, protein and polymer were mixed at the ratio corresponding to maximum turbidity, 5 M NaCl was titrated into the mixture, and the turbidity was measured as a function of salt concentration (Figure 2A and S5C). All tagged proteins phase separated at moderate (near physiological) ionic strength (-9 ~ 100 mM, -12 ~ 150 mM). This represents a 25 – 75 mM increase in salt stability compared to sfGFP with the inclusion of only 3-6 charged amino acids. Detailed experimental results for each GFP variant can be found in Figure S6.

In this case, turbidity decreases with the addition of salt due to a gradual change in the free energy of the system until phase separation is no longer favorable. The increased concentration of free counterions in solution via the addition of salt reduces the release of bound counterions, resulting in smaller entropic gains.[74,77,79] Proteins with increased net

negative charge were expected to be more resistant to salt screening due to stronger electrostatic interactions with the polymer and an increased initial number of bound counterions. Likewise, the sequence defined polypeptide tags were hypothesized to demonstrate varying salt stability due to charge anisotropy or charge patchiness.[67,74,75] This behavior was expected as patchier polypeptides have more confined condensed ions, and thus lower entropy, such that when they are released, the entropy gains are larger.[74] In order to assess these design criteria and the relation to protein concentration in the coacervate phase, the binodal phase boundary of proteins was approximated by measuring the protein concentration in both the coacervate and dilute phases at discrete salt concentrations.

A thorough analysis of protein incorporation in the coacervate was performed to determine the interplay between protein net charge and polypeptide charge patterning. This enabled the construction of phase portraits that accounted for the volume of the coacervate as well as the ionic strength of the initial solution (Figure 2B). This analysis was performed at the macromolecule ratio corresponding to maximum protein concentration in the coacervate with no added salt. Coacervate volumes were determined via overhead fluorescence images where the coacervate droplet was easily identified, thresholded, and analyzed (Figure S7). Tagged GFP variants remained fluorescent through the phase separation process, indicating that the model proteins retained their secondary structure and activity upon concentration in the dense coacervate phase. Consistent with other findings, the preservation of fluorescence suggests that complex coacervation may be capable of incorporating proteins while maintaining their activity, an essential feature for enzyme nanoreactors or therapeutic delivery vehicles.[84–86] Due to the small volume of the condensed phase, it was not possible to measure both the protein and the salt concentration in each phase. It was therefore assumed that the salt concentration

in the two phases were equal. For this reason, tie lines were omitted between each pair of points. While tie lines for other polyelectrolyte complex coacervates have demonstrated slightly negative slopes, a decidedly uneven distribution of salt ions between the two phases would decrease the entropy of mixing and therefore be unlikely.[55,87] Above the ionic strengths displayed for each protein, phase separation did not occur.

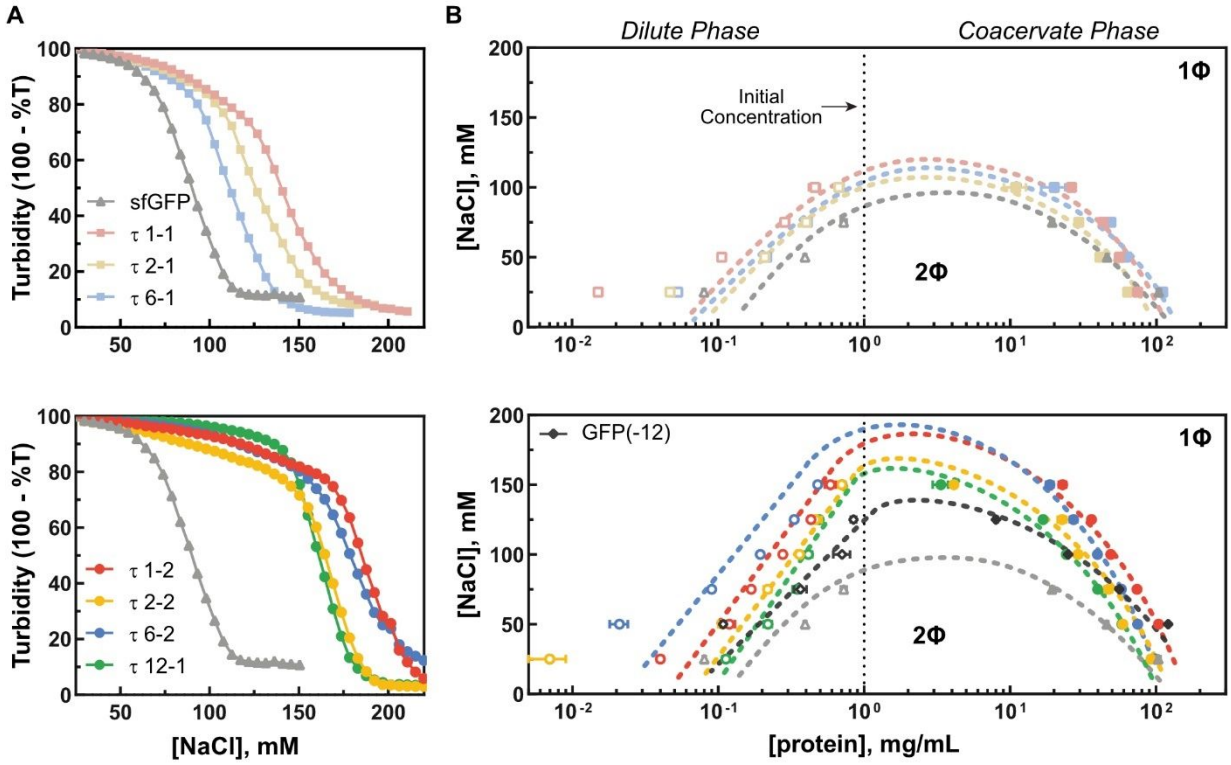

Figure 2. Salt titrations into turbid protein-polymer mixtures (A) and binodal phase portraits (B) for tagged protein library with qP4VP. (Top) Salt titrations and phase portraits for sfGFP and lesser charged mutants (charge = -9). (Bottom) Salt titrations and phase portraits for sfGFP and higher charged mutants (charge = -12). (A) Titration with salt (5 M NaCl, 1 μL increments) to investigate GFP and qP4VP complex dissolution for charged protein mutants compared to sfGFP. (B) Phase portraits for sfGFP and tagged mutants with qP4VP at discrete NaCl concentrations (0*, 25, 50, 75, 100, 125, 150, 200 mM). Protein concentrations in the dilute phase (left) and coacervate phase (right) were determined using fluorescence measurements, using a calibration curve of overhead UV Images to determine the volume of the bulk coacervate phase (Figure S7). Dotted lines approximating the binodal phase boundary are simply a visual aid and do not represent theoretical modeling or analysis. The initial protein concentration of 1 mg mL^{-1} has been represented using a dotted line. *Protein concentrations at 0 mM NaCl have been omitted due to the formation of less-hydrated films, where the volume of the coacervate could not be determined.

Consistently across the library of proteins, the concentration of protein in the coacervate phase decreased as the thermodynamic driving force for dissolution increased (i.e. increasing [NaCl]). sfGFP, -9 charged mutants, and -12 charged mutants phase separated up until salt

concentrations of 75 mM, 100 mM, and 150 mM, respectively – a result consistent with the salt titration data (Figure 2A). For -9 charged mutants (Figure 2B, top), the concentrations of protein in the coacervate phase were comparable for each protein. At the highest salt concentration, more blocky polypeptide tags achieved slightly higher protein concentrations in the coacervate phase, but overall, the tag sequence had minimal effect on coacervation. In this regime, the sfGFP globular domain remains the dominant element as the net charge of the globular domain (-6) is great than that of the polypeptide tag (-3). However, the effect of charge patterning on complex coacervation was expected to be more pronounced for the -12 charged group as the net charge of the polypeptide tag was equal to the net charge of the globular protein domain. These two groupings of the protein variants highlight the interplay between the phase behavior of the globular protein domain and the polypeptide tag sequence. For the -12 charged mutants, at the maximum salt concentration with liquid-liquid phase separation (150 mM), τ 6-2 and τ 1-2 had protein concentrations an order of magnitude higher than the less blocky τ 2-2 and the sterically blocked τ 12-1. The decreased concentration for τ 12-1 was unexpected given the charge blockiness of the polypeptide tag sequence was equivalent to τ 1-2; however, we hypothesize that the addition of six uncharged amino acids at the end of tag sequence results in steric blocking at charged amino acid sites, effectively screening interactions and producing the observed decrease in critical salt concentration. Interestingly, all of the tagged mutants demonstrated an increase in their binodal phase boundary compared to GFP(-12), a sfGFP variant with isotropically distributed charge, reinforcing the notion that charge distribution is an essential design parameter in protein phase separation. To ensure that the dilute and coacervate phases were equilibrated when establishing these phase portraits, the experimental protocol was repeated for protein τ 6-2 using a variety of

equilibration methods (Figure S8). Thermal processing and longer equilibration times did not impact the determined binodal phase boundary significantly, suggesting that the analyzed phase behavior was at or near equilibrium. This phase behavior can be used to tune protein partitioning and stability in complex coacervates. For example, for enzymes with functional active sites, charged tags can potentially be used as a mechanism for protein supercharging without compromising protein structure and activity.

The underlying thermodynamic driving forces for complex coacervation were investigated for a subset of the sfGFP variants by isothermal titration calorimetry (ITC). This technique determines the amount of power that must be supplied to maintain constant temperature as macromolecules interact. As the titration proceeds, the amount of power needed to increase or decrease temperature is indicative of both the sign and magnitude of any interactions taking place, and thus can be used with an appropriate model to calculate thermodynamic properties and affinity constants for the interaction.[74,79,88] Analysis of ITC data was performed using a Two-Step Binding Model previously described by both Priftis et al. and Chang et al, which is separated into two regimes: ion pairing and coacervation, shown in Figure 3A in blue and red, respectively.[74,79] The sum of both contributions is the total energy and was used to fit the data (black). The thermodynamic criteria for complex coacervation is not unique and is common to any spontaneous process. However, the driving force for coacervate formation is unique in that it is system-dependent. While polyelectrolyte-polyelectrolyte coacervation tends to be entropically driven, colloid-polyelectrolyte coacervation can be driven by both entropy gains in the form of counterion release or by electrostatic interactions.[15,77] Predicting a protein's phase behavior thermodynamics would guide the rational design of a charged polypeptide tag given the particular globular protein and polymer,

while also providing guidance for simulations to approximate the phase space of genetically modified globular proteins.

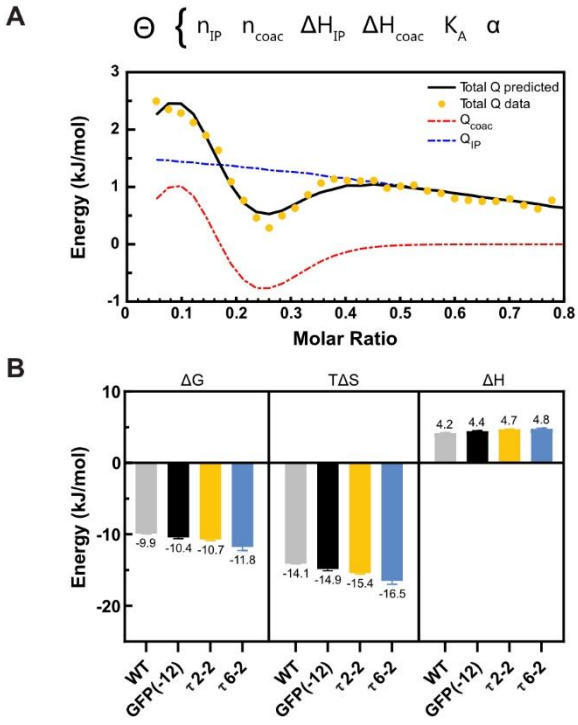

Figure 3. (A) Example (variant: τ 2-2) of fitting ITC data using a two-step binding model with parameter space Θ. Parameter values and individual fits are described in Figure S9. (B) Calculated thermodynamic quantities for each GFP variant during the process of electrostatic attraction and phase separation with qP4VP. Free energy (ΔG), entropy (TΔS), and enthalpy (ΔH) are plotted from left to right. Error bars represent the standard error relative to the mean (N = 3).

ITC was performed for a subset of variants in the library to determine if the observed shift in the binodal curves and salt stability correlated with the system thermodynamics (Figure 3B). The complex coacervation thermodynamics of sfGFP was compared with three of the -12 mutants: τ 2-2, τ 6-2, and the isotropic control GFP(-12) (summarized in Figure S9). These mutants were selected to thermodynamically assess the relative importance of charge distribution (surface or tag) and charge patterning (blocky or regularly distributed) on complex coacervation. Enthalpically, increasing charge and/or charge anisotropy only produced minor

unfavorable changes. As expected in PE-PE systems, entropy was the primary thermodynamic driving force for phase separation and this driving force increased with increasing charge. Anisotropically supercharged variants (i.e. tagged) demonstrated thermodynamic advantages over their isotropic counterparts and these differences were consistent with the trends observed in the titrations and phase portraits shown in Figure 2. Specifically, as the protein net charge increased so did the entropic driving force. When comparing the relative entropic gains compared to sfGFP, τ 6-2 demonstrated a 3-fold increase (2.4 kJ/mol) in its entropic driving force relative to the isotropic GFP(-12) control (0.8 kJ/mol). This shift in thermodynamic driving force is critical to the variant's phase behavior and once again demonstrates that complex coacervation is a multifaceted phenomenon that depends as much, if not more, on charge distribution and not only the protein's net charge. This observation is consistent with trends observed in linear polypeptides, where condensed counterions are confined along with backbone of more charge blocky polypeptides.[74] Here, the increase in thermodynamic driving force was attained using this relationship between charge distribution and confinement effects; together, these modest changes to the protein sequence with a short 12 amino acid polypeptide tag result in a thermodynamic difference that can be used in either linear polypeptides or globular proteins to tune phase behavior.

Conclusions.

The design rules for the complex coacervation of globular proteins were investigated using a library of anionic sfGFP variants tagged with polypeptide sequences consisting of both ionizable and neutral amino acids in different arrangements. Protein supercharging via charged tags required only modest changes to the protein sequence and this method of supercharging did not affect protein yield. Using qP4VP as the cationic counterpart, the phase

behavior of this system was analyzed and optimized. All of the variants underwent complex coacervation with modest, if any, differences in turbidity and encapsulation efficiency at low ionic strength. When interactions were screened with salt, the net charge of sfGFP mutants and the charge distribution within the polypeptide tags synergistically affected the formation and salt stability of complex coacervates. These phase portraits are the first of their kind for engineered protein coacervates, and this thorough evaluation of encapsulation efficiencies indicated that charge distribution has a pronounced effect on globular protein phase behavior, especially at elevated ionic strengths. The charge distribution on the protein surface was not varied or analyzed in this study, but similarly “patchy” protein surface charge distributions have been shown to promote phase separation.[67,89] Isothermal titration calorimetry indicated that the binodal shift in critical salt concentration was due to increased entropic gains upon phase separation. Charge blocky tags like τ 6-2 doubled the critical salt concentration and increased the entropic driving force substantially (2.4 kJ/mol) when compared to GFP without a tag. While these short tags substantially increased the protein net charge, equally charged isotropic counterparts did not demonstrate comparable thermodynamic advantages. The lack of structure-function relationships for the complex coacervation of globular proteins has prevented the theoretical prediction of such thermodynamic data. Moving forward, we hope to help in the collective effort to bridge this gap to better understand, design, and optimize protein phase behavior for a wide-range of applications.

Acknowledgements The authors acknowledge the financial support of the National Science Foundation under award number 1844149. The authors would like to thank the Mass

Spectrometry and PBCF facilities and their directors, Brandon Fowler and Jia Ma, in the Columbia University Department of Chemistry.

Funding Sources N.A.Z. and A.C.O. received funding from the National Science Foundation under award number 1844149.

Supporting Information. (PDF) The supporting information is available free of charge at [ACS website].

- General materials and methods, experimental procedures, experimental data, models, and codes (PDF)

References.

(1) Abbondanzieri, E. A.; Meyer, A. S. More than Just a Phase: The Search for Membraneless Organelles in the Bacterial Cytoplasm. *Curr Genet* **2019**, *65* (3), 691–694. https://doi.org/10.1007/s00294-018-00927-x.

(2) Boeynaems, S.; Alberti, S.; Fawzi, N. L.; Mittag, T.; Polymenidou, M.; Rousseau, F.; Schymkowitz, J.; Shorter, J.; Wolozin, B.; Van Den Bosch, L.; Tompa, P.; Fuxreiter, M. Protein Phase Separation: A New Phase in Cell Biology. *Trends in Cell Biology* **2018**, *28* (6), 420–435. https://doi.org/10.1016/j.tcb.2018.02.004.

(3) McClintock, B. The Relation of a Particular Chromosomal Element to the Development of the Nucleoli in Zea Mays. *Z.Zellforsch* **1934**, *21* (2), 294–326. https://doi.org/10.1007/BF00374060.

(4) Montgomery, T. S. H. Comparative Cytological Studies, with Especial Regard to the Morphology of the Nucleolus. *J. Morphol.* **1898**, *15* (2), 265–582. https://doi.org/10.1002/jmor.1050150204.

(5) Cornejo, E.; Abreu, N.; Komeili, A. Compartmentalization and Organelle Formation in Bacteria. *Current Opinion in Cell Biology* **2014**, *26*, 132–138. https://doi.org/10.1016/j.ceb.2013.12.007.

(6) Jun, S.; Mulder, B. Entropy-Driven Spatial Organization of Highly Confined Polymers: Lessons for the Bacterial Chromosome. *Proceedings of the National Academy of Sciences* **2006**, *103* (33), 12388–12393. https://doi.org/10.1073/pnas.0605305103.

(7) Mitrea, D. M.; Kriwacki, R. W. Phase Separation in Biology; Functional Organization of a Higher Order. *Cell Commun Signal* **2016**, *14* (1), 1. https://doi.org/10.1186/s12964-015-0125-7.

(8) Razin, S. V.; Gavrilov, A. A. The Role of Liquid–Liquid Phase Separation in the Compartmentalization of Cell Nucleus and Spatial Genome Organization. *Biochemistry Moscow* **2020**, *85* (6), 643–650. https://doi.org/10.1134/S0006297920060012.

(9) Murthy, A. C.; Dignon, G. L.; Kan, Y.; Zerze, G. H.; Parekh, S. H.; Mittal, J.; Fawzi, N. L. Molecular Interactions Underlying Liquid−liquid Phase Separation of the FUS Low-Complexity Domain. *Nat Struct Mol Biol* **2019**, *26* (7), 637–648. https://doi.org/10.1038/s41594-019-0250-x.

(10) Yoshizawa, T.; Nozawa, R.-S.; Jia, T. Z.; Saio, T.; Mori, E. Biological Phase Separation: Cell Biology Meets Biophysics. *Biophys Rev* **2020**, *12* (2), 519–539. https://doi.org/10.1007/s12551-020-00680-x.

(11) Paloni, M.; Bailly, R.; Ciandrini, L.; Barducci, A. Unraveling Molecular Interactions in Liquid–Liquid Phase Separation of Disordered Proteins by Atomistic Simulations. *J. Phys. Chem. B* **2020**, *124* (41), 9009–9016. https://doi.org/10.1021/acs.jpcb.0c06288.

(12) Wei, M.-T.; Elbaum-Garfinkle, S.; Holehouse, A. S.; Chen, C. C.-H.; Feric, M.; Arnold, C. B.; Priestley, R. D.; Pappu, R. V.; Brangwynne, C. P. Phase Behaviour of Disordered Proteins Underlying Low Density and High Permeability of Liquid Organelles. *Nature Chem* **2017**, *9* (11), 1118–1125. https://doi.org/10.1038/nchem.2803.

(13) Blocher, W. C.; Perry, S. L. Complex Coacervate-Based Materials for Biomedicine. *WIREs Nanomed Nanobiotechnol* **2017**, *9* (4), e1442. https://doi.org/10.1002/wnan.1442.

(14) Feric, M.; Vaidya, N.; Harmon, T. S.; Mitrea, D. M.; Zhu, L.; Richardson, T. M.; Kriwacki, R. W.; Pappu, R. V.; Brangwynne, C. P. Coexisting Liquid Phases Underlie Nucleolar Subcompartments. *Cell* **2016**, *165* (7), 1686–1697. https://doi.org/10.1016/j.cell.2016.04.047.

(15) Sing, C. E. Development of the Modern Theory of Polymeric Complex Coacervation. *Advances in Colloid and Interface Science* **2017**, *239*, 2–16. https://doi.org/10.1016/j.cis.2016.04.004.

(16) Veis, A. PHASE SEPARATION IN POLYELECTROLYTE SOLUTIONS. II. INTERACTION EFFECTS. *J. Phys. Chem.* **1961**, *65* (10), 1798–1803. https://doi.org/10.1021/j100827a026.

(17) Michaeli, I.; Overbeek, J. Th. G.; Voorn, M. J. Phase Separation of Polyelectrolyte Solutions. *J. Polym. Sci.* **1957**, *23* (103), 443–450. https://doi.org/10.1002/pol.1957.1202310337.

(18) Deshpande, S.; Brandenburg, F.; Lau, A.; Last, M. G. F.; Spoelstra, W. K.; Reese, L.; Wunnava, S.; Dogterom, M.; Dekker, C. Spatiotemporal Control of Coacervate Formation within Liposomes. *Nat Commun* **2019**, *10* (1), 1800. https://doi.org/10.1038/s41467-019-09855-x.

(19) Blocher McTigue, W. C.; Perry, S. L. Design Rules for Encapsulating Proteins into Complex Coacervates. *Soft Matter* **2019**, *15* (15), 3089–3103. https://doi.org/10.1039/C9SM00372J.

(20) Xu, Y.; Mazzawi, M.; Chen, K.; Sun, L.; Dubin, P. L. Protein Purification by Polyelectrolyte Coacervation: Influence of Protein Charge Anisotropy on Selectivity. *Biomacromolecules* **2011**, *12* (5), 1512–1522. https://doi.org/10.1021/bm101465y.

(21) Snead, W. T.; Gladfelter, A. S. The Control Centers of Biomolecular Phase Separation: How Membrane Surfaces, PTMs, and Active Processes Regulate Condensation. *Molecular Cell* **2019**, *76* (2), 295–305. https://doi.org/10.1016/j.molcel.2019.09.016.

(22) Lyon, A. S.; Peeples, W. B.; Rosen, M. K. A Framework for Understanding the Functions of Biomolecular Condensates across Scales. *Nat Rev Mol Cell Biol* **2020**. https://doi.org/10.1038/s41580-020-00303-z.

(23) Yoo, H.; Triandafillou, C.; Drummond, D. A. Cellular Sensing by Phase Separation: Using the Process, Not Just the Products. *Journal of Biological Chemistry* **2019**, *294* (18), 7151–7159. https://doi.org/10.1074/jbc.TM118.001191.

(24) Alberti, S.; Dormann, D. Liquid–Liquid Phase Separation in Disease. *Annu. Rev. Genet.* **2019**, *53* (1), 171–194. https://doi.org/10.1146/annurev-genet-112618-043527.

(25) Spannl, S.; Tereshchenko, M.; Mastromarco, G. J.; Ihn, S. J.; Lee, H. O. Biomolecular Condensates in Neurodegeneration and Cancer. *Traffic* **2019**, *20* (12), 890–911. https://doi.org/10.1111/tra.12704.

(26) Elbaum-Garfinkle, S. Matter over Mind: Liquid Phase Separation and Neurodegeneration. *Journal of Biological Chemistry* **2019**, *294* (18), 7160–7168. https://doi.org/10.1074/jbc.REV118.001188.

(27) Patel, A.; Lee, H. O.; Jawerth, L.; Maharana, S.; Jahnel, M.; Hein, M. Y.; Stoynov, S.; Mahamid, J.; Saha, S.; Franzmann, T. M.; Pozniakovski, A.; Poser, I.; Maghelli, N.; Royer, L. A.; Weigert, M.; Myers, E. W.; Grill, S.; Drechsel, D.; Hyman, A. A.; Alberti, S. A Liquid-to-Solid Phase Transition of the ALS Protein FUS Accelerated by Disease Mutation. *Cell* **2015**, *162* (5), 1066–1077. https://doi.org/10.1016/j.cell.2015.07.047.

(28) Cai, D.; Liu, Z.; Lippincott-Schwartz, J. Biomolecular Condensates and Their Links to Cancer Progression. *Trends in Biochemical Sciences* **2021**, S0968000421000049. https://doi.org/10.1016/j.tibs.2021.01.002.

(29) Le, N. L.; Duong, P. H. H.; Nunes, S. P. 1.6 Advanced Polymeric and Organic–Inorganic Membranes for Pressure-Driven Processes. In *Comprehensive Membrane Science and Engineering*; Elsevier, 2017; pp 120–136. https://doi.org/10.1016/B978-0-12-409547-2.12275-9.

(30) Kim, J. F.; Jung, J. T.; Wang, H.; Drioli, E.; Lee, Y. M. 1.15 Effect of Solvents on Membrane Fabrication via Thermally Induced Phase Separation (TIPS): Thermodynamic and Kinetic Perspectives. In *Comprehensive Membrane Science and Engineering*; Elsevier, 2017; pp 386–417. https://doi.org/10.1016/B978-0-12-409547-2.12690-3.

(31) Zhang, K.; Ma, Y.; Francis, L. F. Porous Polymer/Bioactive Glass Composites for Soft-to-Hard Tissue Interfaces. *J. Biomed. Mater. Res.* **2002**, *61* (4), 551–563. https://doi.org/10.1002/jbm.10227.

(32) Bongiovanni, R.; Vitale, A. Smart Multiphase Polymer Coatings for the Protection of Materials. In *Smart Composite Coatings and Membranes*; Elsevier, 2016; pp 213–234. https://doi.org/10.1016/B978-1-78242-283-9.00008-7.

(33) Goel, M.; Thelakkat, M. Polymer Thermoelectrics: Opportunities and Challenges. *Macromolecules* **2020**, *53* (10), 3632–3642. https://doi.org/10.1021/acs.macromol.9b02453.

(34) Murnen, H. K.; Rosales, A. M.; Jaworski, J. N.; Segalman, R. A.; Zuckermann, R. N. Hierarchical Self-Assembly of a Biomimetic Diblock Copolypeptoid into Homochiral Superhelices. *J. Am. Chem. Soc.* **2010**, *132* (45), 16112–16119. https://doi.org/10.1021/ja106340f.

(35) Rosales, A. M.; Segalman, R. A.; Zuckermann, R. N. Polypeptoids: A Model System to Study the Effect of Monomer Sequence on Polymer Properties and Self-Assembly. *Soft Matter* **2013**, *9* (35), 8400. https://doi.org/10.1039/c3sm51421h.

(36) Lam, C. N.; Yao, H.; Olsen, B. D. The Effect of Protein Electrostatic Interactions on Globular Protein–Polymer Block Copolymer Self-Assembly. *Biomacromolecules* **2016**, *17* (9), 2820–2829. https://doi.org/10.1021/acs.biomac.6b00522.

(37) Lindhoud, S.; Claessens, M. M. A. E. Accumulation of Small Protein Molecules in a Macroscopic Complex Coacervate. *Soft Matter* **2016**, *12* (2), 408–413. https://doi.org/10.1039/C5SM02386F.

(38) Lee, Y.; Ishii, T.; Cabral, H.; Kim, H. J.; Seo, J.-H.; Nishiyama, N.; Oshima, H.; Osada, K.; Kataoka, K. Charge-Conversional Polyionic Complex Micelles-Efficient Nanocarriers for Protein Delivery into Cytoplasm. *Angewandte Chemie International Edition* **2009**, *48* (29), 5309–5312. https://doi.org/10.1002/anie.200900064.

(39) Kim, A.; Miura, Y.; Ishii, T.; Mutaf, O. F.; Nishiyama, N.; Cabral, H.; Kataoka, K. Intracellular Delivery of Charge-Converted Monoclonal Antibodies by Combinatorial Design of Block/Homo Polyion Complex Micelles. *Biomacromolecules* **2016**, *17* (2), 446–453. https://doi.org/10.1021/acs.biomac.5b01335.

(40) Mills, C. E.; Obermeyer, A.; Dong, X.; Walker, J.; Olsen, B. D. Complex Coacervate Core Micelles for the Dispersion and Stabilization of Organophosphate Hydrolase in Organic Solvents. *Langmuir* **2016**, *32* (50), 13367–13376. https://doi.org/10.1021/acs.langmuir.6b02350.

(41) Jaturanpinyo, M.; Harada, A.; Yuan, X.; Kataoka, K. Preparation of Bionanoreactor Based on Core−Shell Structured Polyion Complex Micelles Entrapping Trypsin in the Core Cross-Linked with Glutaraldehyde. *Bioconjugate Chem.* **2004**, *15* (2), 344–348. https://doi.org/10.1021/bc034149m.

(42) Crosby, J.; Treadwell, T.; Hammerton, M.; Vasilakis, K.; Crump, M. P.; Williams, D. S.; Mann, S. Stabilization and Enhanced Reactivity of Actinorhodin Polyketide Synthase Minimal Complex in Polymer–Nucleotide Coacervate Droplets. *Chem. Commun.* **2012**, *48* (97), 11832. https://doi.org/10.1039/c2cc36533b.

(43) Water, J. J.; Schack, M. M.; Velazquez-Campoy, A.; Maltesen, M. J.; van de Weert, M.; Jorgensen, L. Complex Coacervates of Hyaluronic Acid and Lysozyme: Effect on Protein Structure and Physical Stability. *European Journal of Pharmaceutics and Biopharmaceutics* **2014**, *88* (2), 325–331. https://doi.org/10.1016/j.ejpb.2014.09.001.

(44) Davis, B. W.; Aumiller, W. M.; Hashemian, N.; An, S.; Armaou, A.; Keating, C. D. Colocalization and Sequential Enzyme Activity in Aqueous Biphasic Systems: Experiments and Modeling. *Biophysical Journal* **2015**, *109* (10), 2182–2194. https://doi.org/10.1016/j.bpj.2015.09.020.

(45) Veis, A. A Review of the Early Development of the Thermodynamics of the Complex Coacervation Phase Separation. *Advances in Colloid and Interface Science* **2011**, *167* (1–2), 2–11. https://doi.org/10.1016/j.cis.2011.01.007.

(46) Sariban, A.; Binder, K. Critical Properties of the Flory–Huggins Lattice Model of Polymer Mixtures. *The Journal of Chemical Physics* **1987**, *86* (10), 5859–5873. https://doi.org/10.1063/1.452516.

(47) Bernstein, R. E.; Cruz, C. A.; Paul, D. R.; Barlow, J. W. LCST Behavior in Polymer Blends. *Macromolecules* **1977**, *10* (3), 681–686. https://doi.org/10.1021/ma60057a037.

(48) Li, N. K.; Quiroz, F. G.; Hall, C. K.; Chilkoti, A.; Yingling, Y. G. Molecular Description of the LCST Behavior of an Elastin-Like Polypeptide. *Biomacromolecules* **2014**, *15* (10), 3522–3530. https://doi.org/10.1021/bm500658w.

(49) Roberts, S.; Dzuricky, M.; Chilkoti, A. Elastin-like Polypeptides as Models of Intrinsically Disordered Proteins. *FEBS Letters* **2015**, *589* (19PartA), 2477–2486. https://doi.org/10.1016/j.febslet.2015.08.029.

(50) Ruff, K. M.; Roberts, S.; Chilkoti, A.; Pappu, R. V. Advances in Understanding Stimulus-Responsive Phase Behavior of Intrinsically Disordered Protein Polymers. *Journal of Molecular Biology* **2018**, *430* (23), 4619–4635. https://doi.org/10.1016/j.jmb.2018.06.031.

(51) Lin, Y.-H.; Forman-Kay, J. D.; Chan, H. S. Theories for Sequence-Dependent Phase Behaviors of Biomolecular Condensates. *Biochemistry* **2018**, *57* (17), 2499–2508. https://doi.org/10.1021/acs.biochem.8b00058.

(52) Tian, Y.; Booth, J.; Meehan, E.; Jones, D. S.; Li, S.; Andrews, G. P. Construction of Drug–Polymer Thermodynamic Phase Diagrams Using Flory–Huggins Interaction Theory: Identifying the Relevance of Temperature and Drug Weight Fraction to Phase Separation within Solid Dispersions. *Mol. Pharmaceutics* **2013**, *10* (1), 236–248. https://doi.org/10.1021/mp300386v.

(53) Radhakrishna, M.; Basu, K.; Liu, Y.; Shamsi, R.; Perry, S. L.; Sing, C. E. Molecular Connectivity and Correlation Effects on Polymer Coacervation. *Macromolecules* **2017**, *50* (7), 3030–3037. https://doi.org/10.1021/acs.macromol.6b02582.

(54) Andreev, M.; Prabhu, V. M.; Douglas, J. F.; Tirrell, M.; de Pablo, J. J. Complex Coacervation in Polyelectrolytes from a Coarse-Grained Model. *Macromolecules* **2018**, *51* (17), 6717–6723. https://doi.org/10.1021/acs.macromol.8b00556.

(55) Li, L.; Srivastava, S.; Andreev, M.; Marciel, A. B.; de Pablo, J. J.; Tirrell, M. V. Phase Behavior and Salt Partitioning in Polyelectrolyte Complex Coacervates. *Macromolecules* **2018**, *51* (8), 2988–2995. https://doi.org/10.1021/acs.macromol.8b00238.

(56) Andreev, M.; Chremos, A.; de Pablo, J.; Douglas, J. F. Coarse-Grained Model of the Dynamics of Electrolyte Solutions. *J. Phys. Chem. B* **2017**, *121* (34), 8195–8202. https://doi.org/10.1021/acs.jpcb.7b04297.

(57) Fredrickson, G. H.; Ganesan, V.; Drolet, F. Field-Theoretic Computer Simulation Methods for Polymers and Complex Fluids. *Macromolecules* **2002**, *35* (1), 16–39. https://doi.org/10.1021/ma011515t.

(58) Samanta, R.; Ganesan, V. Influence of Protein Charge Patches on the Structure of Protein–Polyelectrolyte Complexes. *Soft Matter* **2018**, *14* (46), 9475–9488. https://doi.org/10.1039/C8SM01535J.

(59) Wang, R.; Wang, Z.-G. On the Theoretical Description of Weakly Charged Surfaces. *The Journal of Chemical Physics* **2015**, *142* (10), 104705. https://doi.org/10.1063/1.4914170.

(60) Zhang, P.; Shen, K.; Alsaifi, N. M.; Wang, Z.-G. Salt Partitioning in Complex Coacervation of Symmetric Polyelectrolytes. *Macromolecules* **2018**, *51* (15), 5586–5593. https://doi.org/10.1021/acs.macromol.8b00726.

(61) Shen, K.; Wang, Z.-G. Polyelectrolyte Chain Structure and Solution Phase Behavior. *Macromolecules* **2018**, *51* (5), 1706–1717. https://doi.org/10.1021/acs.macromol.7b02685.

(62) Longo, G. S.; Olvera de la Cruz, M.; Szleifer, I. Molecular Theory of Weak Polyelectrolyte Gels: The Role of PH and Salt Concentration. *Macromolecules* **2011**, *44* (1), 147–158. https://doi.org/10.1021/ma102312y.

(63) Shakya, A.; Girard, M.; King, J. T.; Olvera de la Cruz, M. Role of Chain Flexibility in Asymmetric Polyelectrolyte Complexation in Salt Solutions. *Macromolecules* **2020**, *53* (4), 1258–1269. https://doi.org/10.1021/acs.macromol.9b02355.

(64) Perry, S. L.; Sing, C. E. PRISM-Based Theory of Complex Coacervation: Excluded Volume versus Chain Correlation. *Macromolecules* **2015**, *48* (14), 5040–5053. https://doi.org/10.1021/acs.macromol.5b01027.

(65) Gomes, E.; Shorter, J. The Molecular Language of Membraneless Organelles. *Journal of Biological Chemistry* **2019**, *294* (18), 7115–7127. https://doi.org/10.1074/jbc.TM118.001192.

(66) Obermeyer, A. C.; Mills, C. E.; Dong, X.-H.; Flores, R. J.; Olsen, B. D. Complex Coacervation of Supercharged Proteins with Polyelectrolytes. *Soft Matter* **2016**, *12* (15), 3570–3581. https://doi.org/10.1039/C6SM00002A.

(67) Kapelner, R. A.; Obermeyer, A. C. Ionic Polypeptide Tags for Protein Phase Separation. *Chem. Sci.* **2019**, *10* (9), 2700–2707. https://doi.org/10.1039/C8SC04253E.

(68) Cummings, C. S.; Obermeyer, A. C. Phase Separation Behavior of Supercharged Proteins and Polyelectrolytes. *Biochemistry* **2018**, *57* (3), 314–323. https://doi.org/10.1021/acs.biochem.7b00990.

(69) Uversky, V. N.; Kuznetsova, I. M.; Turoverov, K. K.; Zaslavsky, B. Intrinsically Disordered Proteins as Crucial Constituents of Cellular Aqueous Two Phase Systems and Coacervates. *FEBS Letters* **2015**, *589* (1), 15–22. https://doi.org/10.1016/j.febslet.2014.11.028.

(70) Molliex, A.; Temirov, J.; Lee, J.; Coughlin, M.; Kanagaraj, A. P.; Kim, H. J.; Mittag, T.; Taylor, J. P. Phase Separation by Low Complexity Domains Promotes Stress Granule Assembly and Drives Pathological Fibrillization. *Cell* **2015**, *163* (1), 123–133. https://doi.org/10.1016/j.cell.2015.09.015.

(71) Babu, M. M. The Contribution of Intrinsically Disordered Regions to Protein Function, Cellular Complexity, and Human Disease. *Biochemical Society Transactions* **2016**, *44* (5), 1185–1200. https://doi.org/10.1042/BST20160172.

(72) Brangwynne, C. P.; Eckmann, C. R.; Courson, D. S.; Rybarska, A.; Hoege, C.; Gharakhani, J.; Julicher, F.; Hyman, A. A. Germline P Granules Are Liquid Droplets That Localize by Controlled Dissolution/Condensation. *Science* **2009**, *324* (5935), 1729–1732. https://doi.org/10.1126/science.1172046.

(73) Pak, C. W.; Kosno, M.; Holehouse, A. S.; Padrick, S. B.; Mittal, A.; Ali, R.; Yunus, A. A.; Liu, D. R.; Pappu, R. V.; Rosen, M. K. Sequence Determinants of Intracellular Phase Separation by Complex Coacervation of a Disordered Protein. *Molecular Cell* **2016**, *63* (1), 72–85. https://doi.org/10.1016/j.molcel.2016.05.042.

(74) Chang, L.-W.; Lytle, T. K.; Radhakrishna, M.; Madinya, J. J.; Vélez, J.; Sing, C. E.; Perry, S. L. Sequence and Entropy-Based Control of Complex Coacervates. *Nat Commun* **2017**, *8* (1), 1273. https://doi.org/10.1038/s41467-017-01249-1.

(75) Madinya, J. J.; Chang, L.-W.; Perry, S. L.; Sing, C. E. Sequence-Dependent Self-Coacervation in High Charge-Density Polyampholytes. *Mol. Syst. Des. Eng.* **2020**, *5* (3), 632–644. https://doi.org/10.1039/C9ME00074G.

(76) Statt, A.; Casademunt, H.; Brangwynne, C. P.; Panagiotopoulos, A. Z. Model for Disordered Proteins with Strongly Sequence-Dependent Liquid Phase Behavior. *J. Chem. Phys.* **2020**, *152* (7), 075101. https://doi.org/10.1063/1.5141095.

(77) Kayitmazer, A. B. Thermodynamics of Complex Coacervation. *Advances in Colloid and Interface Science* **2017**, *239*, 169–177. https://doi.org/10.1016/j.cis.2016.07.006.

(78) Priftis, D.; Tirrell, M. Correction: Phase Behaviour and Complex Coacervation of Aqueous Polypeptide Solutions. *Soft Matter* **2015**, *11* (2), 422–422. https://doi.org/10.1039/C4SM90162B.

(79) Priftis, D.; Laugel, N.; Tirrell, M. Thermodynamic Characterization of Polypeptide Complex Coacervation. *Langmuir* **2012**, *28* (45), 15947–15957. https://doi.org/10.1021/la302729r.

(80) Chollakup, R.; Beck, J. B.; Dirnberger, K.; Tirrell, M.; Eisenbach, C. D. Polyelectrolyte Molecular Weight and Salt Effects on the Phase Behavior and Coacervation of Aqueous Solutions of Poly(Acrylic Acid) Sodium Salt and Poly(Allylamine) Hydrochloride. *Macromolecules* **2013**, *46* (6), 2376–2390. https://doi.org/10.1021/ma202172q.

(81) Samanta, R.; Halabe, A.; Ganesan, V. Influence of Charge Regulation and Charge Heterogeneity on Complexation between Polyelectrolytes and Proteins. *J. Phys. Chem. B* **2020**, *124* (22), 4421–4435. https://doi.org/10.1021/acs.jpcb.0c02007.

(82) Perry, S.; Li, Y.; Priftis, D.; Leon, L.; Tirrell, M. The Effect of Salt on the Complex Coacervation of Vinyl Polyelectrolytes. *Polymers* **2014**, *6* (6), 1756–1772. https://doi.org/10.3390/polym6061756.

(83) Kayitmazer, A. B.; Koksal, A. F.; Kilic Iyilik, E. Complex Coacervation of Hyaluronic Acid and Chitosan: Effects of PH, Ionic Strength, Charge Density, Chain Length and the Charge Ratio. *Soft Matter* **2015**, *11* (44), 8605–8612. https://doi.org/10.1039/C5SM01829C.

(84) Nolles, A.; Westphal, A.; Kleijn, J.; van Berkel, W.; Borst, J. Colorful Packages: Encapsulation of Fluorescent Proteins in Complex Coacervate Core Micelles. *IJMS* **2017**, *18* (7), 1557. https://doi.org/10.3390/ijms18071557.

(85) Sureka, H. V.; Obermeyer, A. C.; Flores, R. J.; Olsen, B. D. Catalytic Biosensors from Complex Coacervate Core Micelle (C3M) Thin Films. *ACS Appl. Mater. Interfaces* **2019**, *11* (35), 32354–32365. https://doi.org/10.1021/acsami.9b08478.

(86) Mi, X.; Blocher McTigue, W. C.; Joshi, P. U.; Bunker, M. K.; Heldt, C. L.; Perry, S. L. Thermostabilization of Viruses *via* Complex Coacervation. *Biomater. Sci.* **2020**, *8* (24), 7082–7092. https://doi.org/10.1039/D0BM01433H.

(87) Jha, P.; Desai, P.; Li, J.; Larson, R. PH and Salt Effects on the Associative Phase Separation of Oppositely Charged Polyelectrolytes. *Polymers* **2014**, *6* (5), 1414–1436. https://doi.org/10.3390/polym6051414.

(88) Sing, C. E.; Perry, S. L. Recent Progress in the Science of Complex Coacervation. *Soft Matter* **2020**, *16* (12), 2885–2914. https://doi.org/10.1039/D0SM00001A.

(89) Kim, S.; Sureka, H. V.; Kayitmazer, A. B.; Wang, G.; Swan, J. W.; Olsen, B. D. Effect of Protein Surface Charge Distribution on Protein–Polyelectrolyte Complexation. *Biomacromolecules* **2020**, *21* (8), 3026–3037. https://doi.org/10.1021/acs.biomac.0c00346.